Linewidth Control and the Improved Adhesion of Inkjet-Printed Ag on Polyimide Substrate, Textured Using Near-Atmospheric Pressure Plasmas

Mu Kyeom Mun, Jin Woo Park, Geun Young Yeom*

In this paper, the effect of polyimide surface modification – using near-atmospheric pressure plasmas – on the line width and adhesion of inkjet-printed Ag was investigated by texturing and modifying the chemical composition of the polyimide surface. The polyimide surface was textured with He/O_2, to increase the surface area of the polyimide substrate and it increased the water contact angle from 57 to 137°, when the textured polyimide surface was treated with a SF_6 plasma after the texturing process. The textured polyimide surface also exhibited the increased adhesion strength of Ag film (by about two times), due to the increase in the contact area, as expected, according to the Wenzel model. The linewidth of the inkjet-printed Ag line decreased by about ten times from 330 μm (for the flat polyimide surface) to 23 μm (for the textured polyimide surface) in addition to having smoother line edges.

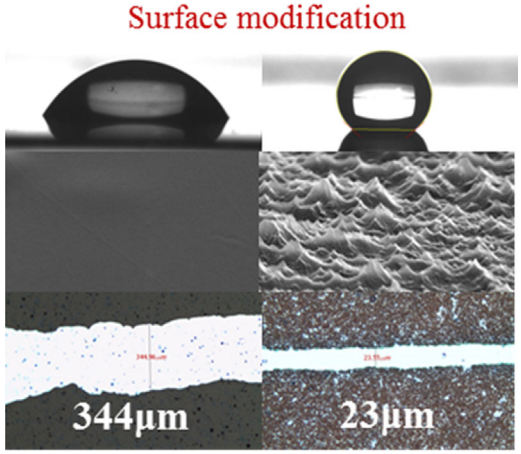

1. Introduction

Micro-patterning is widely used in the production of semiconductor devices, flat panel display devices, sensor devices, and so forth.[1–4] In general, in order to pattern a material, the material is etched in a vacuum chamber, using reactive plasmas or wet etchants after the photolithographic patterning of the materials surface with a photoresist.[5,6] However, the conventional indirect patterning (using photolithography) is not only a complicated process, but also an expensive one; therefore, except for nanoscale semiconductor device processing, various direct patterning techniques, like screen printing, gravure printing, and inkjet printing are investigated.[7–9]

Direct patterning has advantages in mass production, such as in-line and roll-to-roll processing;[10] due to the use of low temperatures,[11] it also can be applicable to polymer substrates, which are being intensively investigated as potential substrates for the next generation of flexible displays, wearable computers, and other electronic devices.[12] Many direct printing methods (such as screen, gravure, and inkjet printing) are being investigated; among these, contact printing methods – like screen and gravure printing—demonstrate a tendency to inflict some damage on the substrate and consume excessive ink in the printing process. Inkjet printing has advantages over the other direct printing techniques, due to the characteristic of being non-contact, and also because of its efficient use of ink.[13–15] However, in

M. K. Mun, J. W. Park, G. Y. Yeom
School of Advanced Materials Science and Engineering, Sungkyunkwan University, Suwon, Kyunggi-do 16419, South Korea
E-mail: gyyeom@skku.edu

Plasma Process. Polym. **2016,** DOI: 10.1002/ppap.201500222
© 2016 WILEY-VCH Verlag GmbH & Co. KGaA, Weinheim

Early View Publication; these are NOT the final page numbers, use DOI for citation !!

inkjet printing there is an inherent difficulty involved in controlling the linewidth of the ink on the substrate while increasing the adhesion of the printed materials to the substrate. That is, when the substrate surface is treated to be hydrophobic in order to control the linewidth, the adhesion strength of the inkjet printed material to the substrate is decreased.[16–19] On the other hand, when the substrate surface is treated to become hydrophilic for the increased adhesion of the inkjet printed materials to the substrate, the control of linewidth of the ink is decreased. [20,21]

In our previous study, regarding Ag inkjet printing on polymer substrates, both the control of the linewidth and an increase in the adhesion of the ink could be obtained through micro-masking and selectively etching the polymer substrate surface by using atmospheric pressure plasmas; that is, by texturing the polymer substrate surface.[22] By increasing the surface area coming in contact with the Ag ink by texturing (as suggested by the Wenzel model),[23] while making the substrate surface hydrophobic, controlling the Ag ink linewidth while simultaneously improving the adhesion to the substrate was possible. However, the texturing process used previously is complicated, due to the use of SiO_x for micromasking; the micromask layer needs to be removed after the texturing. In addition, the atmospheric pressure plasma may not be easily applicable to the actual substrate processing, due to the difficulty in controlling the gas environment and in using various reactive gas combinations.

Therefore, in this study, the texturing of the polymer surface was conducted using sprayed graphene flakes as a micromask layer, and by using a near atmospheric pressure (~500 Torr) plasma; the effect of this method on both the linewidth control and the adhesion of the Ag ink to the polyimide substrate was investigated. Graphene flakes, sprayed on the polyimide substrate, were used as an etch mask layer to improve the possibility of in-line processing because it is also etched during the texturing process, and the remaining graphene flake residue could be easily removed by wet cleaning. The near-atmospheric pressure plasma was used to process the substrates easily, employing either an in-line a roll-to-roll process; it was also used for easier scalability to large area processing while keeping the process gas environment similar to the low pressure processing.[23,24]

2. Methods

2.1. Near Atmospheric Pressure Plasma System and Process

The plasma system used in this study is shown in Figure 1; it is a double discharge source, composed of a remote plasma source on the top and a direct plasma source at the bottom.

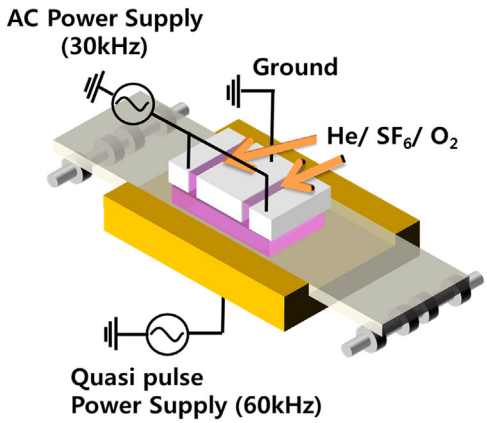

Figure 1. A schematic diagram of the near atmospheric pressure plasma system used in the experiment. The plasma source was a double-discharge source, composed of a remote plasma source and a direct plasma source, and operated at 500 Torr.

The remote plasma source was operated by applying 30 kHz AC voltage to the top two electrodes, located on the outsides, while the top center electrode was grounded. In addition, 60 kHz AC voltage was applied to the bottom electrode to form a direct plasma while operating the remote plasma. We used the double discharge source as the plasma source to operate the plasma more stably and with higher densities. All the electrodes were made of aluminum, the outside of which was coated with a 400 μm thick Al_2O_3 dielectric barrier, via thermal spraying. The length of the two top ground electrodes was 50 mm and the length of the top center power electrode was 70 mm. The gap between the upper electrodes (for the remote plasma) is 2 mm, and the gap between the top electrodes and bottom electrode (for the direct plasma) is 1 mm.

A gas mixture of He/O_2 and He/SF_6 was fed from the top side along the gap of the top electrodes. The operating pressure was kept at a little lower than the atmospheric pressure of 500 Torr by using a vacuum chamber-type system, to maintain gas safety, process gas purity, external environment, and process reproducibility. The polyimide substrate (150 μm thick; DuPont) was transported between the top electrodes and bottom electrodes at the fixed velocity of 0.3 m min^{-1}. With this plasma condition, the etch rate of the polyimide was about 390 nm/min and no significant surface roughness was observed on the etched polyimide surface when etched without graphene mask.

2.2. Graphene Mask Spray Process

To texture the polyimide surface, graphene flakes (XG sciences, C-300; It consists of aggregates of sub-micron platelets that have a particle diameter of less than two

© 2016 WILEY-VCH Verlag GmbH & Co. KGaA, Weinheim

Early View Publication; these are NOT the final page numbers, use DOI for citation !!

microns and a typical particle thickness of a few nanometers, depending on the surface area. Grade C-300 particles have the average surface areas of 300 m^2/g.) were applied as the etch mask; the graphene-flake-covered polyimide surface was etched by the double discharge source, with He/O_2. We used graphene flakes as the etch mask because it is generally cheaper than other mask materials, can be applied using the spray-coating method, and can be easily cleaned with water. In order to create the etch mask, the flakes were dispersed in isopropanol and sprayed into the air onto the polyimide film using a spray gun, as shown in Figure 2 (Fuso Seiki, GP-2). The graphene flakes were not pretreated to prevent from aggregation. Figure 2 also shows the SEM images of the polyimide substrate surface (a) before and (b) after the graphene spray-coated on it. The density of the graphene flakes on the polyimide surface was estimated by measuring the optical transmittance of the polyimide covered with the flakes.

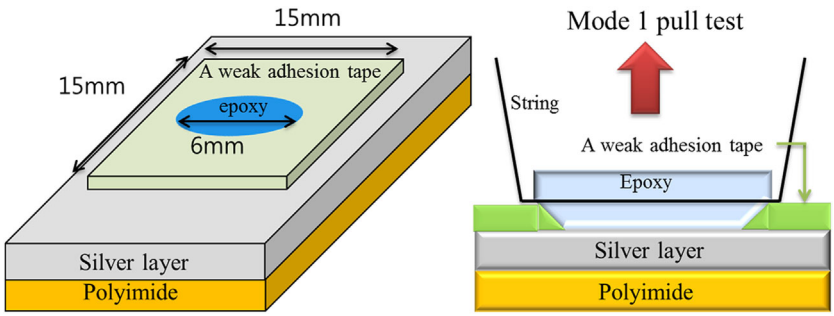

Figure 3. The sample configuration used to measure the adhesion force of Ag film spraycoated on the textured polyimide film. A weak adhesion tape (DAIO, ES5810) with 15 mm of each side and a hole of 6 mm diameter was taped in the middle of the silver layer surface. The exposed 6 cm diameter Ag surface was glued to a string, using an epoxy for the Mode I pull test.

2.3. Specimen Preparation for Adhesion Test

To measure the adhesion force of the Ag ink coating on the plasma textured polyimide surface, a commercial Ag ink (AMOGREENTECH, B-30) was spin coated on the textured polyimide for 30 s the speed of 2000 rpm, and then the Ag ink was sintered (by soft-baking at 150 °C for 30 min, and hard-baking at 200 °C for an hour). After the sintering, as shown in Figure 3, a weak adhesion tape (DAIO, ES5810) with 15 mm on each side and a hole of 6 mm diameter was taped in the middle of the Ag layer surface. The exposed 6 mm diameter Ag surface was glued to a string using an epoxy for the Mode I pull test (vertical opening test).[25] The weak adhesion film with a hole over the Ag layer was used to limit the test area so that it was exactly the same for different samples during the adhesion test. The adhesion force was measured with a tensile strength tester (MECMESIN, Multi test 1-i).

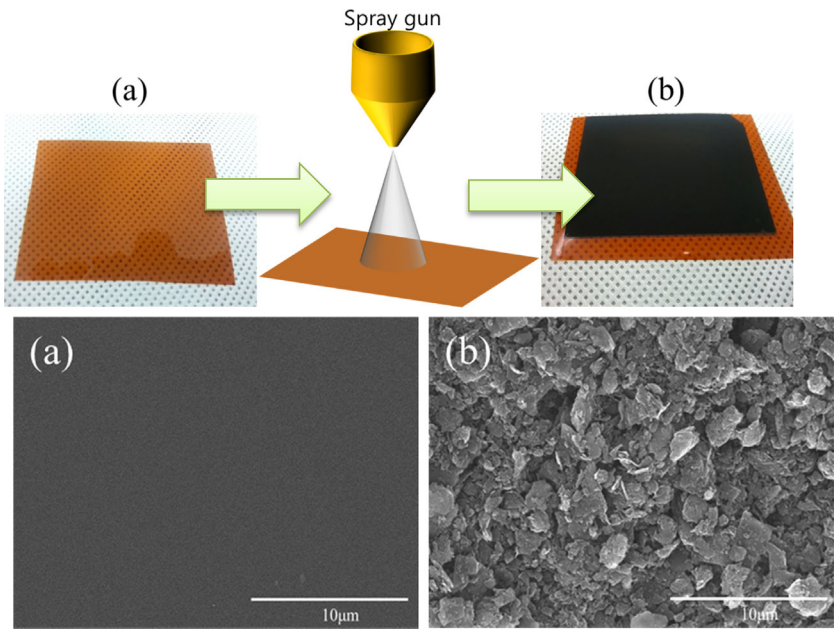

Figure 2. The optical and SEM images, showing polyimide film (a) before and (b) after the graphene flake spray-coating on the polyimide surface.

2.4. Direct Inkjet Process

To measure the change of inkjet-printed Ag linewidth before and after the plasma texturing, the Ag ink was printed on the textured polyimide surface using a piezoelectric-type inkjet printer (FUJIFILM Dimatix materials printer, DMP-2800) and an ink cartridge, using the bend mode (Dimatix DMC-11610 cartridge). The cartridge printer height was 250 μm and the ink dot spacing was set at 20 μm. The jetting frequency was 1 kHz, and the pulse duration was 11.58 μs, to enable the Ag ink to jet without a tail and satellite.

2.5. Analysis and Measurements

The density of the graphene flake mask was estimated using an ultraviolet/visible (UV/VIS) spectrophotometer (Shimadzu, UV-3600) because the morphology of the polyimide surface after

© 2016 WILEY-VCH Verlag GmbH & Co. KGaA, Weinheim

Early View Publication; these are NOT the final page numbers, use DOI for citation !!

etching with the He/O_2 plasma is dependent on the graphene flake mask density. The surface area (per the projected area), after the texturing using the He/O_2 plasma, was estimated by measuring the surface morphology with an atomic force microscope (AFM, Veeco, 849-012-711), and by calculating the surface area using software (Gwyddion 2.35). The water contact angle on the polyimide surface, before and after the plasma treatments, was measured using a contact angle analyzer (SEO, phoenix 450). The chemical composition of the polyimide surface, after the various plasma treatments, was measured using an X-ray photoelectron spectroscopy (XPS, thermo VG SIGMA PROBE). The surface morphology, after plasma texturing, was measured using a scanning electron microscope (FE-SEM, HITACHI, S-4700).

3. Results and Discussion

To increase the surface area of the polyimide, the surface was masked with graphene flakes and etched using a He/O_2 plasma. Figure 4(b) shows one of the SEM images after the graphene flake was spray-coated on the flat polyimide surface, as in Figure 4(a). The density of graphene on the polyimide surface having the 20% optical transmittance (see Figure 5) was used. To texture the polyimide surface masked with the graphene flakes, a double-discharge composed of a remote plasma operated at 6 kV and a direct plasma operated at 6 kV was used with the He (6 slm)/O_2 (1 slm), while transporting the substrate at the speed of 0.3 m min^{-1}. The substrate was exposed to the plasma for two minutes. During the He/O_2 plasma exposure, the polyimide area not covered by the graphene flakes was etched. In the case of the polyimide area covered with graphene flakes, the size of the graphene flake was decreased by the etching of the graphene flakes with the oxygen plasma, and the newly exposed polyimide surface was also etched by the oxygen plasmas. Therefore, after the He/O_2 plasma exposure, as shown in Figure 4(c), a textured polyimide surface with a small amount of graphene residue was obtained. The graphene residue was washed away easily with water, possibly due to the formation of hydrophilic graphene oxide during the etching.[26] After the cleaning, the polyimide surface showed a clean textured surface as illustrated in Figure 4(d).

The density of the graphene flake on the polyimide surface affects the degree of texturing – that is, it changes the surface area of the polyimide surface after the texturing. Figure 5 shows the effect of the graphene mask density on the surface morphology, and the change in the surface area of the polyimide after etching with the He/O_2 plasma, in Figure 4. As an indicator of the graphene mask density on the polyimide surface, the optical transmittance of the polyimide surface covered with graphene flakes was measured using the UV/VIS spectrophotometer. The lower the optical transmittance, the greater the coverage of graphene flakes on the polyimide surface, as shown in the top SEM images of Figure 5. The second line of SEM images in Figure 5 illustrates the polyimide surfaces after texturing with the He/O_2 plasma. As a result of the decreasing optical transmittance, due to the increase of the graphene flake coverage, the degree of surface texturing was increased. However, when the optical transmittance was lower than 20%, due to the opening area of the polyimide surface being too small, the degree of surface texturing was decreased. The surface morphology of the textured surface was measured using AFM, and the actual surface area was calculated (with the AFM data) using the software, Gwyddion. The changed surface area percentage of the textured polyimide, compared to the smooth surface measured as a function of the optical transmittance, is shown in the bottom portion of Figure 5. As shown in Figure 5, the surface area of the polyimide was increased, thus, decreasing the optical transmittance and showing a maximum of 23.7% at an optical transmittance of 20%; the further decrease in the optical transmittance lowered the previously increased surface area.

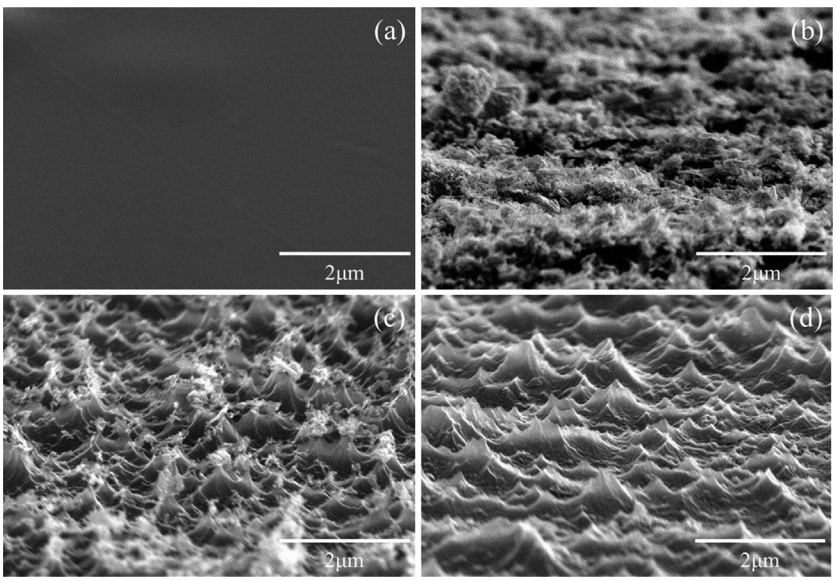

Figure 4. SEM images of the polyimide surface (a) before graphene flake coating, (b) after the graphene flake coating as the etch mask for polyimide texturing, (c) after the texturing the polyimide surface using a He/O_2 plasma with the graphene flake residue, (d) after the removal of graphene flake residue by water washing.

© 2016 WILEY-VCH Verlag GmbH & Co. KGaA, Weinheim
DOI: 10.1002/ppap.201500222

↖ Early View Publication; these are NOT the final page numbers, use DOI for citation !!

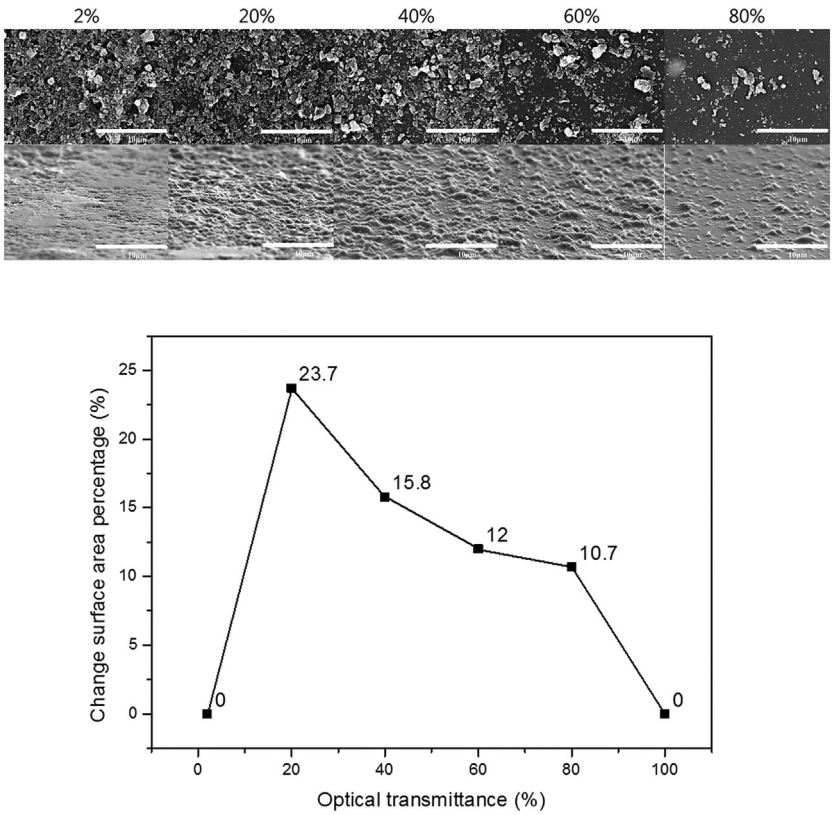

Figure 5. The effect of the graphene mask density on the surface morphology, and on the change in the surface area of polyimide after the texturing with the He/O_2 plasma. The SEM images in the first and second line show the images of the polyimide surface after masking with different densities of graphene flakes, and after the texturing with the He/O_2 plasma, respectively. The bottom figure shows the changed surface area percentage of the textured polyimide, compared to the smooth surface measured as a function of the optical transmittance of the polyimide covered with graphene flakes.

Texturing the polyimide surface with graphene flake not only changed the surface area but also changed the composition of the etched surface. While the surface composition of the polyimide area (covered with graphene flake) remains same as before, the area textured by the He/O_2 plasma changed the surface composition by exposing the surface to oxygen radicals and ions. The change in the mask density changes the area of textured polyimide surface; as such, the overall surface composition of the etched polyimide surface can be changed with the mask density. To separate the effect of the surface composition and texturing on the contact angle and the adhesion of the Ag ink, the effect of different gas plasma treatments on the surface composition and the contact angle was investigated using a flat polyimide surface. Figure 6 shows the effect of plasma treatments, using He/SF_6 and He/O_2, using flat non-masked polyimide surfaces, on the contact angle. O_2 flow rates (1–4 slm) and SF_6 flow rates (0.2–0.8 slm) were varied while keeping the He flow rates at 6 slm. The voltages to the remote plasma source and the direct plasma source varied from 4 to 6 kV, with the samples being exposed to the plasma for two minutes. (Therefore, when the voltage to the remote plasma source was 4 kV, the voltage to the direct plasma source was also kept at 4kV; 4–4kV.) When the polyimide surface was exposed to the He/O_2 plasma, the contact angle decreased, and a lower contact angle was observed at the higher voltages. However, when the polyimide surface was exposed to the He/SF_6 plasma, the contact angle increased and a higher contact angle was observed at the higher voltage. The gas flow rates of the O_2 and SF_6 did not change the contact angle noticeably.

Table 1 shows the chemical composition, measured using XPS, for the polyimide surface treated with He (6 slm)/O_2 (1 slm) and He (6 slm)/SF_6 (0.6 slm) at 6 kV AC voltage for two minutes. After the He/O_2 plasma treatment, the increase of percentage of oxygen on the polyimide surface was observed, indicating the formation of more hydrophilic C—O bondings, which results in the decrease of contact angle, while (after the He/SF6 plasma treatment) an F percentage close to 34.6% was observed as a result of the formation of hydrophobic C—F bondings which, in turn, resulted in the increase of the contact angle as shown in Figure 6.

To obtain the same surface composition on the textured polyimide surfaces as the other surface areas, and, thus, remove the effect of the surface composition on the contact angle for the variously textured polyimide surfaces, these surfaces were treated with the same plasma, and the contact angles were measured. The results are shown in Figure 7. In particular, to obtain a higher contact angle, the textured polyimide surfaces were treated with the same He (6 slm)/SF_6 (0.6 slm), at 6 kV of AC voltages, for two minutes. Table 1 also shows the surface composition of the textured polyimide surface (20% transmittance), after the He/SF6 plasma treatment. As shown in the table, the surface composition of the textured polyimide surface was almost the same as that of the flat polyimide surface (100% transmittance) treated with the same plasma. Therefore, it is believed that all of the textured polyimide surfaces have a similar surface composition after the same He/SF6 plasma treatment. As shown in Figure 7, even though the surface

© 2016 WILEY-VCH Verlag GmbH & Co. KGaA, Weinheim

Early View Publication; these are NOT the final page numbers, use DOI for citation !!

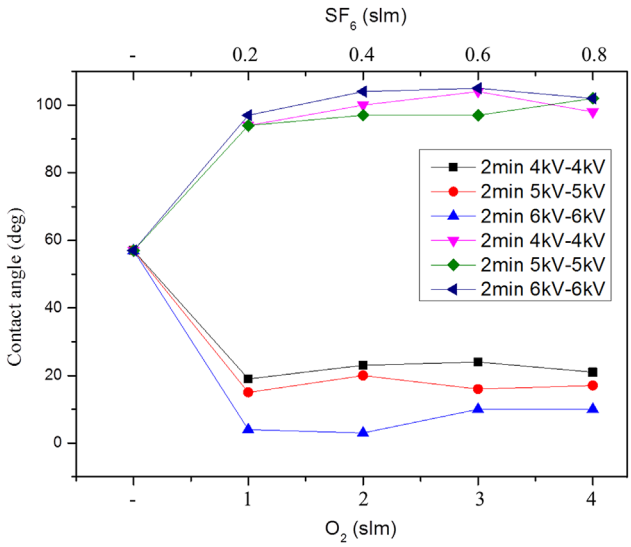

Figure 6. The effect of the plasma treatment on flat, non-masked, polyimide surfaces using He/SF6 and He/O_2 on the contact angle. The O_2 flow rates (1–4 slm) and SF_6 flow rates (0.2–0.8 slm) were varied while flowing 6 slm of He. The voltages to the remote plasma source and direct plasma source varied from 4 to 6 kV and the samples were exposed to the plasma for two minutes.

compositions were similar for the variously textured polyimides, the contact angle changed with the degree of texturing and, when compared with Figure 5, it can be determined that the increased surface area also increases the contact angle.

When the surface is textured, the contact interface is determined by the Cassie–Baxter model or the Wenzel model.[27,28] The Cassie–Baxter model is observed when the roughness is significantly high and the water contact angle is increased, with the increase of surface roughness through the formation of an air pocket between the substrate and the water droplet. The Wenzel model is observed when the surface roughness is not significantly high, and the water contact angle is also increased with the increase of surface area by the following equations.[27,28] For a flat surface, the surface tensions are balanced and the stable contact angle of (θ_c) is formed by Equation (1):

$$A = \gamma_1 - \gamma_{12} = \gamma_2 \cos\theta_c \quad (1)$$

where A is the adhesion tension, γ_1 is the interface tension on between substrate and the air, γ_{12} is the interface tension on between the water droplet and air, γ_2 is the interface tension on between the substrate and the water droplet, and the θ_c is the equilibrium contact angle of the water droplet on the substrate. By texturing the surface, the surface area is increased and, in this case, the equation is changed to Equation (2). Equation (2), using the Wenzel model, shows that the increasing actual surface area (r) increases the contact angle (θ_c'):[29,30]

$$rA = r(\gamma_1 - \gamma_{12}) = \gamma_2 \cos\theta_c' \quad (2)$$

$$r = \text{roughness factor} = \frac{\text{actualsurfacearea}}{\text{projectedsurfacearea}} \quad (3)$$

In addition, in the case of the Cassie–Baxter model, by increasing the surface roughness, the decrease of adhesion between two interfaces is observed as the Lotus effect. However, in the case of the Wenzel model, the contact area

Table 1. The surface composition of the polyimide, measured using XPS for as-is, flat polyimide treated with a He/O_2 plasma, flat polyimide (no graphene mask) and textured polyimide (using the graphene flakes with 20% transmittance) treated with a He/SF_6 plasma. For the plasma treatments, He (6 slm)/O_2 (1 slm) and He (6 slm)/SF_6 (0.6 slm) at 6 kV AC voltages were used for two minutes.

Operating condition	C	O	N	F
As-is	68.5	23.3	8.2	–
He/O_2 flat	61.6	29.7	8.7	–
He/SF_6				
Transmittance 100% (Flat)	43.6	16.5	5.3	34.6
Transmittance 20% (Roughened)	43.9	16.2	5.3	34.6

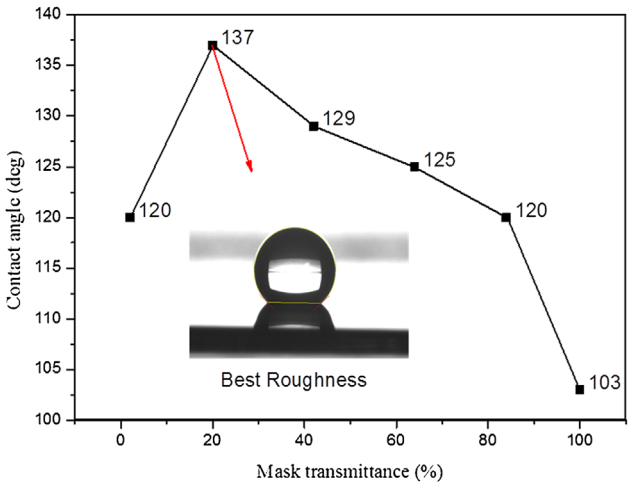

Figure 7. The effect of the graphene mask transmittance of the polyimide surface on the contact angle of the textured polyimide. After texturing the polyimide surface, to obtain a higher contact angle, the textured polyimide surfaces were treated with the same He (6 slm)/SF_6 (0.6 slm) at 6 kV of AC voltages for two minutes.

© 2016 WILEY-VCH Verlag GmbH & Co. KGaA, Weinheim

↖ Early View Publication; these are NOT the final page numbers, use DOI for citation !!

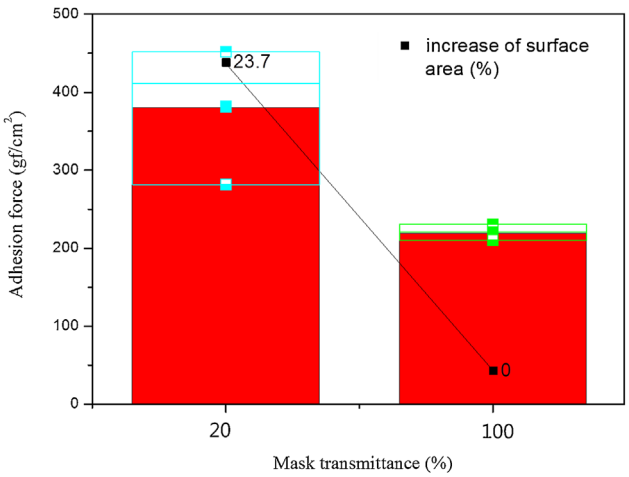

Figure 8. The adhesion force between the polyimide substrate and the Ag film, formed by spin-coated Ag ink, using the method shown in Figure 3. Polyimide surfaces textured with the He/O_2 plasma for the optical transmittance of 20 and 100% (flat) were used for the adhesion test. Before the Ag ink spin-coating, the textured polyimide surfaces were treated with an He/SF_6 plasma for the same surface compositions shown in Table 1.

is increased with the greater texturing, and the adhesion strength between the interfaces is also increased with greater surface texturing.[27,28] On the polyimide surface, the differences in the adhesion strength, with and without the surface texturing, was investigated by measuring the adhesion force between the polyimide substrate and the Ag ink. spin-coated on the polyimide surfaces using the measurement method shown in Figure 3. The results are shown in Figure 8. The polyimide surfaces textured with the He/O_2 plasma, for an optical transmittance of 20 and 100% (flat), were used for the adhesion test. Before the Ag ink spin coating, the textured polyimide surfaces were treated with the He/SF_6 plasma, to have the similar surface composition as that shown in Table 1. As shown in Figure 8, as the Wenzel model expected, the adhesion force between the Ag and polyimide substrate increased by about two times from 210 to 400 gf/cm^2 after the surface texturing (with the graphene flake of 20% transmittance).

When the Wenzel model is applied, not only the increase of adhesion strength but also the increase of contact angle is expected. Using an Ag inkjet, an Ag line was printed on both the textured polyimide surface (20% transmittance, 23.7% increased surface area) and the flat polyimide surface (100% transmittance) in Figure 8, using an inkjet printer. The results, on SEM images of the printed Ag lines, are shown in Figure 9. By texturing the polyimide surface (that is, by increasing the surface area about 23.7%), for the same surface composition, a decrease in the Ag linewidth (from 330 to 23 μm) and a smoother line edge could be observed. If we use an inkjet with initially smaller dots/lines, it is believed that a much smaller and smoother Ag linewidth could be obtained after the texturing the polyimide surface.

4. Conclusion

The polyimide surface was modified using $He/O_2/SF_6$ near-atmospheric pressure plasmas, and the effect of the surface texturing on the adhesion of the Ag film on the polyimide surface (and the linewidth control of the inkjet-printed Ag line) was investigated. For the texturing the polyimide surface, the surface – which was spray-coated with graphene flakes – was treated with He/O_2 plasmas. The surface texturing changed with the graphene flake density, and the highest texturing (corresponding to a 23.7% increase in the actual surface area) was observed when graphene-flake-coated polyimide had 20% transmittance. The change in the water contact angle was related to the change in the actual surface area via the texturing, and the highest water contact angle (137°) was observed at the highest polyimide surface area, when the surface composition of the textured polyimide surfaces was made similar by being treated with an He/SF6 plasma. The He/SF6 plasma was used to increase the contact angle, by making the polyimide surface hydrophobic. When the graphene flakes were spray-coated on the textured polyimide surface (23.7% increased surface area), the increased adhesion strength of the Ag film on the textured polyimide surface, by about two times compared to flat polyimide surface, could be observed; this indicates that the Wenzel model can be applied to the interface between the Ag ink and textured

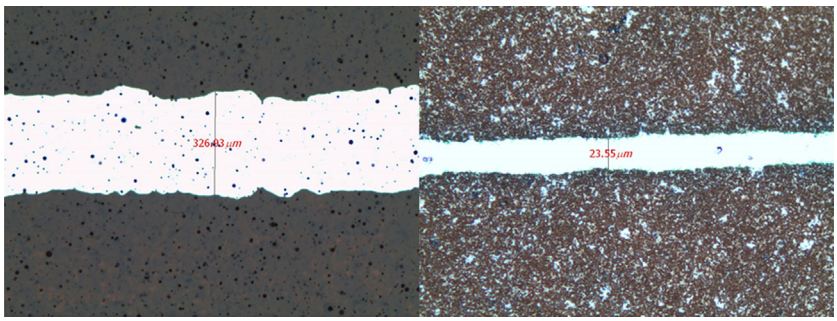

Figure 9. The optical microscope images of the Ag lines inkjet-printed on the textured polyimide surface (20% transmittance, 23.7% increased surface area), and the flat polyimide surface (100% transmittance) shown in Figure 8, using an inkjet printer.

© 2016 WILEY-VCH Verlag GmbH & Co. KGaA, Weinheim

Early View Publication; these are NOT the final page numbers, use DOI for citation !!

polyimide substrate. When Ag inkjet printing was performed on the polyimide surfaces, the decrease of the Ag linewidth from 330 μm for the flat polyimide to 23 μm (and smoother line edge) for the textured polyimide (23.7% increased surface area) could be observed. It is believed that the polyimide texturing method used in this study can be applied to control the linewidth and improve the adhesion strength of Ag lines inkjet-printed on the flexible substrate cheaply and reliably as an in-line system, which is required for the next generation of flexible electronic device fabrication.

Acknowledgements: This work was carried out through a project supported by Samsung Electro-Mechanics, to improve adhesive force using modified atmospheric-pressure plasma (S-2014-1507-0011).

Received: December 10, 2015; Revised: January 25, 2016; Accepted: January 25, 2016;DOI: 10.1002/ppap.201500222

Keywords: direct patterning; flexible device; inkjet printing; near-atmospheric pressure plasma; surface modification

[1] C. A. Aguilar, Y. Lu, S. Mao, S. Chen, *Biomaterials* **2005**, *26*, 7642.
[2] F. F. Amos, S. A. Morin, J. A. Streifer, R. J. Hamers, S. Jin, *J. Am. Chem. Soc.* **2007**, *129*, 14296.
[3] K. Autumn, M. Sitti, Y. A. Liang, A. M. Peattie, W. R. Hansen, S. Sponberg, T. W. Kenny, R. Fearing, J. N. Israelachvili, R. J. Full, *Proc. Natl. Acad. Sci. U. S. A.* **2002**, *99*, 12252.
[4] Z. Burton, B. Bhushan, *Nano Lett.* **2005**, *5*, 1607.
[5] J. Choi, Y. Kim, S. Lee, S. U. Son, H. S. Ko, V. D. Nguyen, D. Byun, *Appl. Phys. Lett.* **2008**, *93*, 193508.
[6] J. S. Choi, K. Y. Cho, J. Yim, *Eur. Polym. J.* **2010**, *46*, 389.
[7] B. De Gans, U. S. Schubert, *Langmuir* **2004**, *20*, 7789.
[8] K. Itoga, M. Yamato, J. Kobayashi, A. Kikuchi, T. Okano, *Biomaterials* **2004**, *25*, 2047.
[9] D. Jang, D. Kim, B. Lee, S. Kim, M. Kang, D. Min, J. Moon, *Adv. Funct. Mater.* **2008**, *18*, 2862.
[10] S. Jung, M. Dorrestijn, D. Raps, A. Das, C. M. Megaridis, D. Poulikakos, *Langmuir* **2011**, *27*, 3059.
[11] T. Kawase, T. Shimoda, C. Newsome, H. Sirringhaus, R. H. Friend, *Thin Solid Films* **2003**, *438*, 279.
[12] S. H. Ko, H. Pan, C. P. Grigoropoulos, C. K. Luscombe, J. M. Fréchet, D. Poulikakos, *Nanotechnology* **2007**, *18*, 345202.
[13] M. Laroussi, X. Lu, *Appl. Phys. Lett.* **2005**, *87*, 113902.
[14] T. Lee, Y. Choi, S. Nam, C. You, D. Na, H. Choi, D. Shin, K. Kim, K. Jung, *Thin Solid Films* **2008**, *516*, 7875.
[15] E. Menard, M. A. Meitl, Y. Sun, J. Park, D. J. Shir, Y. Nam, S. Jeon, J. A. Rogers, *Chem. Rev.* **2007**, *107*, 1117.
[16] J. Noh, M. Jung, K. Jung, G. Lee, S. Lim, D. Kim, S. Kim, J. M. Tour, G. Cho, *Org. Electron.* **2011**, *12*, 2185.
[17] H. Pan, Y. Li, Y. Wu, P. Liu, B. S. Ong, S. Zhu, G. Xu, *J. Am. Chem. Soc.* **2007**, *129*, 4112.
[18] J. Puetz, M. A. Aegerter, *Thin Solid Films* **2008**, *516*, 4495.
[19] D. Qin, Y. Xia, G. M. Whitesides, *Nat. Protoc.* **2010**, *5*, 491.
[20] M. A. Sarshar, C. Swarctz, S. Hunter, J. Simpson, C. Choi, *Colloid Polym. Sci.* **2013**, *291*, 427.
[21] A. Shimoni, S. Azoubel, S. Magdassi, *Nanoscale* **2014**, *6*, 11084.
[22] J. B. Park, J. Y. Choi, S. H. Lee, Y. S. Song, G. Y. Yeom, *Soft Matter.* **2012**, *8*, 5020.
[23] K. Shin, J. Hong, J. Jang, *Adv. Mater.* **2011**, *23*, 2113.
[24] H. Sirringhaus, T. Kawase, R. H. Friend, T. Shimoda, M. Inbasekaran, W. Wu, E. P. Woo, *Science* **2000**, *290*, 2123.
[25] K. Friedrich, R. Walter, L. Carlsson, A. Smiley, J. Gillespie Jr., *J. Mater. Sci.* **1989**, *24*, 3387.
[26] Z. Wang, J. Zhang, R. Xing, J. Yuan, D. Yan, Y. Han, *J. Am. Chem. Soc.* **2003**, *125*, 15278.
[27] R. N. Wenzel, *Ind. Eng. Chem.* **1936**, *28*, 988.
[28] S. Yoo, T. Lho, D. C. Seok, Y. C. Hong, B. Lee, *Thin Solid Films* **2011**, *519*, 6746.
[29] Q. Yu, Z. Zeng, W. Zhao, H. Li, X. Wu, Q. Xue, *Chem. Commun.* **2013**, *49*, 2424.
[30] K. Zhang, V. Dwivedi, C. Chi, J. Wu, *J. Hazard. Mater.* **2010**, *182*, 162.

© 2016 WILEY-VCH Verlag GmbH & Co. KGaA, Weinheim

↖ **Early View Publication; these are NOT the final page numbers, use DOI for citation !!**